Journal of Solid State Electrochemistry (2023) 27:991–999
https://doi.org/10.1007/s10008-023-05411-2

ORIGINAL PAPER

Fabrication and characterization of graphene/sulfonated polyether sulfone octyl sulfonamide hybrid film with improved proton conductivity performance

Walid Mabrouk[1] · Sonia Jebri[2] · Khaled Charradi[3] · Bishir Silimi[3] · Abdullah Y. A. Alzahrani[4] · Ali Boubakri[1] · Ouassim Ghodbane[5] · Noureddine Raouafi[6] · Sherif. M. A. S. Keshk[3]

Received: 2 December 2022 / Revised: 22 January 2023 / Accepted: 24 January 2023 / Published online: 30 January 2023

Abstract

In this study, graphene (G) was blended with sulfonated polyether sulfone octyl sulfonamide (SPESOS) in different ratios (1, 1.5, and 2 wt.%) to enhance the proton conductivity of SPESOS. The results of the water absorption analysis and current impedance spectroscopy of a G/SPESOS hybrid film showed that the proton conductivity improved due to the hydrophilic-hydrophobic nature of the hybrid. Further analysis showed that the synthesized hybrid film had a desirable contact angle and good ion exchange capacity, water absorption, and thermal stability. The hybrid film with 2 wt.% graphene showed better proton conductivity (92 mS/cm) than the pristine SPESOS film (34 mS/cm) at 100% relative humidity. These results suggested that the synthesized hybrid films offered superior proton conductivity, ion exchange capacity, and hydrophilicity compared to pristine SPESOS.

Keywords Proton conductivity · Graphene · SPESOS film · Hybrid film · Fuel cells

Introduction

The problem of leakage current in internal combustion engines can be solved by using fuel cells, which transform chemical energy into electrical energy. Fuel cells can also decrease environmental pollution by producing little or no greenhouse gases [1–3]. Proton exchange film fuel cells (PEMFCs) are the most suitable power sources for portable and stationary devices due to their high power density, silent operation, quick start, and quiet shutdown [4, 5]. A crucial constituent of PEMFC is the proton exchange film (PEF), which acts as a barrier between the fuel and oxidant, and transfers protons from the anode to the cathode [6]. An ideal PEM should have rapid proton conductivity, low fuel permeability, prolonged morphological stability, high mechanical modulus, and durability under harsh working

Highlights
- An organic-inorganic hybrid film having potential applications in fuel cells was prepared and characterized.
- Graphene improved the contact angle, water uptake, and other physicochemical properties of hybrid films.
- Hybrid film 2% G/SPESOS exhibited proton conductivity augmentation at elevated temperatures and humidity.

✉ Walid Mabrouk
w.mabroukcerte@gmail.com

[1] CERTE, Laboratory Water, Films and Biotechnology of the Environment, Water Research and Technologies Center, Technologic Park Borj Cedria, BP 273, Soliman 8020, Tunisia

[2] CERTE, Laboratory of Desalination and Valorization of Natural Water, Water Research and Technologies Center, Technologic Park Borj Cedria, BP 273, Soliman 2020, Tunisia

[3] CRTEn, Nanomaterials and Systems for Renewable Energy Laboratory, Research and Technology Center of Energy, Technopark Borj Cedria, BP 095 Hammam Lif, Tunisia

[4] KUU, Department of Chemistry, Faculty of Science and Arts, King Khalid University, Mohail Assir, Saudi Arabia

[5] INRAP, National Institute of Research and Physico-Chemical Analysis, Laboratory of Materials, Treatment, and Analysis (LMTA), Sidi Thabet 2020, Tunisia

[6] FST, Laboratory of Analytical Chemistry and Electrochemistry, LR99ES15, University of Tunis El Manar Campus, Tunis 2092, Tunisia

conditions [7]. Hydrocarbon proton-conducting films have been considered to be an alternative to PEM [8]. Polyarylenes can tolerate oxidation and are mechanically strong with comparatively high glass transition temperatures (T_g). Polyarylene ether ketones (PEEK) [9–11] and polyarylene ether sulfones (PES) [12] have been intensively investigated. By functionalizing these polymers via sulfonation, improved film characteristics such as greater wettability, higher water flux, and better perm selectivity can be obtained. Polyether sulfone thermoplastic films are commonly used in reverse osmosis, ultra-filtration, and dialysis, and exhibit high resistance to hydrolysis. This resistance with the simplicity of chemical modification and ease of solution casting makes this polymer a better choice. Polyether sulfone thermoplastic films show a wide range of proton conductivity and water absorptivity depending on the quantity of incorporated octylamine. However, they have certain drawbacks such as SPES (1.3 H^+ pmu) alone is soluble in water at high temperatures and butoctylamine in pristine sulfonated polyether sulfone reduces the solubility of SPESOS in water.

SPESOS films are smooth and have variable ionic conductivities and water uptake capacities, which can be tuned by the amount of incorporated octylamine [13]. The proton conductivity of PEMs generally depends on proton mobility, which is responsible for the enhanced proton conductivity of the hydrated films. Many approaches have been proposed to improve the proton conductivity and mechanical properties of the SPESOS films, and the most common approach is the incorporation of inorganic particles [14, 15]. Compared to pristine SPESOS, SPESOS films modified using sepiolite clay with nanoarchitecture showed higher water retention, lower contact angle, and enhanced proton conductivity [16, 17]. SPESOS hybrid film modified with montmorillonite clay also showed higher proton conductivity. Several other hybrid films based on clays and conducting polymers have also been extensively explored as supercapacitor electrodes. However, only materials based on carbon have desirable flexibility and can be used as self-supporting soft electrodes [18]. The suitability of carbon nanotubes as electrode materials has been established [19]. However, these carbon-based materials have some limitations due to the high capacitance conferred by the unavailability of an active surface. This limitation can be overcome by including an electrochemically active second phase in carbon-based electrodes [20]. Graphene (G), consisting of single-atom thick layers of sp^2-hybridized carbon atoms arranged in a honeycomb lattice, is a promising material for PEMFCs. It is also very strong, light, and thin. A single square-meter sheet of graphene weighs just 0.0077 g but can sustain up to 4 kg [21]. It also has a huge surface area, excellent heat and electrical conductivity, and exceptional electrochemical and mechanical capabilities, which are similar to those of carbon nanotubes [22]. G/polymer nanohybrid fuel cell films possess good proton and electron conductivity with anti-methanol crossover capabilities [23]. Due to its unique electronic structure, it is difficult to disperse pristine graphene in the polymer matrix to produce an atomically well-dispersed nanohybrid.

However, a study described a simple blending process to produce G/PVA nanohybrids resulting in increased ionic conductivity and homogeneously well-connected ionic channels [24]. Poly(diallyl dimethylammonium chloride) (PDDA)/G nanohybrids were also synthesized and compared to a pure graphene electrode (0.25 V). The results showed an exceptional onset potential of 0.15 V (vs. SCE), better fuel selectivity, anti-CO poisoning capabilities, and good stability [25]. A 3D monolithic G/polyaniline (PANi) anode was used in a microbial fuel cell (MFC). A higher power yield (up to 768 mW/m^2) was produced by the 3D graphene/PANi anode-functioned MFC compared to a carbon-cloth anode (158 mW/m^2) [26]. A hybrid of sulfonated poly(ether ketone) (SPEEK) and G was prepared. This hybrid displayed a retentive discharge time of 61 h above 0.8 V [27]. The poor conductivity and limited flexibility of the SPESOS polymer limit its applications in PEMFCs [13]. The effect of graphene on the SPESOS film remains undetermined. To improve water retention and proton conductivity, we performed fast and efficient fabrication of a hybrid film made of SPESOS matrix and graphene nanosheets, in which the graphene nanosheets were well-dispersed in the matrix. The hybrid films were analyzed using Fourier transform infrared (FTIR) spectroscopy, X-ray diffraction (XRD), and thermogravimetry. The contact angles, ion exchange capacities, water absorptivity, and proton conductivity (up to 110 °C) were also determined.

Experimental protocol

Materials and chemicals

Sulfonated polyether sulfone octyl sulfonamide (SPESOS) was synthesized at Eras Labo. Graphene solution was obtained from Angstron Materials (OH, USA). N, N′-dimethylacetamide (DMAc), sulfuric acid, and sodium hydroxide were purchased from Acros Company.

Fabrication of the hybrid films

The hybrid films were prepared using various concentrations of graphene by solution casting followed by evaporation. Different weight percentages (0, 1, 1.5, and 2 wt.%) of graphene (G) were placed in 20 mL of dimethylacetamide and stirred magnetically for 12 h, followed by stirring under ultrasound for 6 h. SPESOS (1.0 g) was dissolved in the same solvent and added to a beaker containing graphene suspension and stirred for 2 h. The resulting polymer solution was sonicated for 10 min until no air bubbles were

observed. This mixture was then poured onto a clean Teflon plate ($S = 100$ cm^2) and heat treated in an oven at different temperatures for different periods [16, 17]. The fabricated membranes were stored separately in closed bags.

Characterization of the films

Fourier transform infrared (FT-IR)

A Nicolet spectrophotometer was used to perform the FT-IR analysis of SPESOS and various hybrid films in the transmission mode.

X-ray diffraction (XRD)

An automated Bruker D8 advance X-ray machine was used for recording the X-ray diffractograms in the 2θ mode between 5 and 80°. The interradicular distance (d) was calculated using Bragg's law as

$$2d \sin \theta = n \lambda$$

Here, θ indicates half of the deviation, d indicates interreticular distance, n indicates an integer called "diffraction order," and λ indicates the wavelength of the X-rays.

Thermogravimetric analysis (TGA)

A Mettler thermogravimetric analyzer was used to record thermograms of the samples. Samples weighing ~3 mg were vacuum dried at 100 °C for 24 h before the analysis. The thermograms were recorded over a temperature range from ambient temperature to 700 °C at a sweep rate of 10 °C/min and an argon flow rate of 40 mL/min [28].

Water uptake (WU)

To determine water absorptivity, the dried films were soaked in deionized water for 2 days at room temperature. Then, the films were weighed after the removal of excess surface water [29]. The water uptake (WU) capacity was calculated using the following formula:

$$\boldsymbol{WU} = \frac{\boldsymbol{W_{wet}} - \boldsymbol{W_{dry}}}{\boldsymbol{W_{dry}}} * 100 \quad (1)$$

Here, W_{wet} and W_{dry} indicate the weights of wet and dry films, respectively.

Contact angle (CA)

A theta optical tensiometer (Attention) was used to measure the contact angle (CA) of the films. A micro-syringe was used to place a droplet (5 µL) of deionized water on the surface of the film (1.5 cm × 1.5 cm). A camera was positioned behind the sample before taking a picture of the water droplet [29]. The contact angle was determined using the Theta attention computer software as soon as there was no discernible change in the surface.

Ion exchange capacity (IEC)

IEC was measured by immersing the films in the acid form ($S = 25$ cm^2) in a sodium hydroxide solution at a concentration of 10^{-2} M for 2 days, thus allowing for complete neutralization. The ion exchange capacity was established by acid–base analysis [30].

The IEC of each film was expressed as meq of sulfonic groups/g of dry polymer and was determined by the following relationship:

$$\boldsymbol{IEC} = \frac{\boldsymbol{n^i_{NaOH}} - \boldsymbol{n^f_{NaOH}}}{\boldsymbol{W_{dry}}} \quad (2)$$

Here, n^{i}_{NaOH} and n^{f}_{NaOH} indicate the initial and the final mol numbers of sodium hydroxide in the solution, respectively, and W_{dry} indicates the dry weight of the film.

Proton conductivity

The proton conductivity of the films was determined by electrochemical impedance spectroscopy at different temperatures and 100% relative humidity (RH) using a VSP potentiostat (BioLogic Science Instruments). Frequency response analysis (FRA) was performed over a frequency range between 1000 kHz and 10 Hz with an oscillating voltage amplitude of 10 mV to record high-frequency Nyquist plots. Electrical resistance (R) was evaluated from the intersection of the high-frequency arc and the axis of real Z_r using the Z view software [31, 32]. Proton conductivity (σ, mS/cm) was evaluated using the following relationship:

$$\boldsymbol{\sigma(mS/cm)} = \frac{\boldsymbol{e}}{\boldsymbol{R \times S}} \quad (3)$$

Here, e denotes the thickness of the film placed between the two electrodes, S denotes the surface area, and R denotes the electrical resistance.

Results and discussion

The graphene sheets had enough surface area for adsorbing SPESOS. Additionally, a strong interfacial contact (π–π stacking) between graphene and aromatic polymer matrix formed a hybrid with better characteristics (Fig. 1) [28].

This can be explained by the development of noncovalent π–π stacking between the basal planes of graphene and the phenyl groups of SPESOS chains (Fig. 1). We found that a slow self-assembly process could result in a stacking interaction. Thus, solution casting followed by evaporation-induced self-assembly is a useful technique for achieving strong interfacial interactions. The features of the hybrids of graphene and SPESOS were significantly affected by these strong interfaces to assist stress dispersion and transfer performance [33, 34].

Fourier transform infrared spectroscopy

The FT-IR spectra of SPESOS and different G/SPESOS films over the range of 500–4000 cm^{-1} are shown in Fig. 2.

The SPESOS film showed a band at 3426 cm^{-1} owing to the O–H vibration, which was significantly broadened after graphene was incorporated into the hybrid films. The two SPESOS distinctive bands that corresponded to the aromatic carbons at 1482 and 1590 cm^{-1} and to the asymmetrical and symmetrical vibrations of O=S=O at 1020 and 1090 cm^{-1} became weaker in hybrid films [29]. These observations indicated that noncovalent π–π stacking occurred between the phenyl groups of SPESOS chains and basal planes of graphene [33, 34].

X-ray diffractogram

The crystalline structures of graphene and hybrid films were revealed by XRD diffractograms, and the resulting data is shown in Fig. 3.

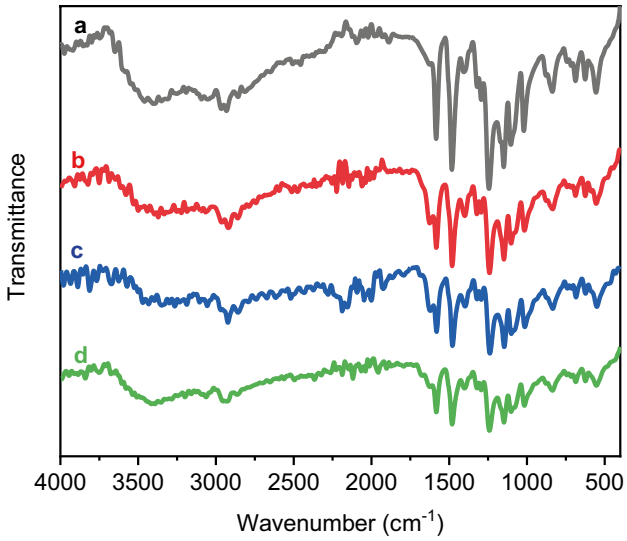

Fig. 2 The FT-IR spectra of **a** SPESOS, **b** 1 wt.% G/SPESOS, **c** 1.5 wt.% G/SPESOS, and **d** 2 wt.% G/SPESOS hybrid films

For SPESOS, abroad peak was observed at $2\theta = 19.17°$ corresponding to the 110 reflection plane and a broad, amorphous peak at about $2\theta = 28.6°$ corresponding to the 002 reflection plane that ensures the presence of SO_3H groups on SPESOS chains [35].

When graphene was added to the SPESOS matrix, the intensity of the diffraction peak corresponding to the 110 plane parallel to the surface of the hybrid increased and shifted to

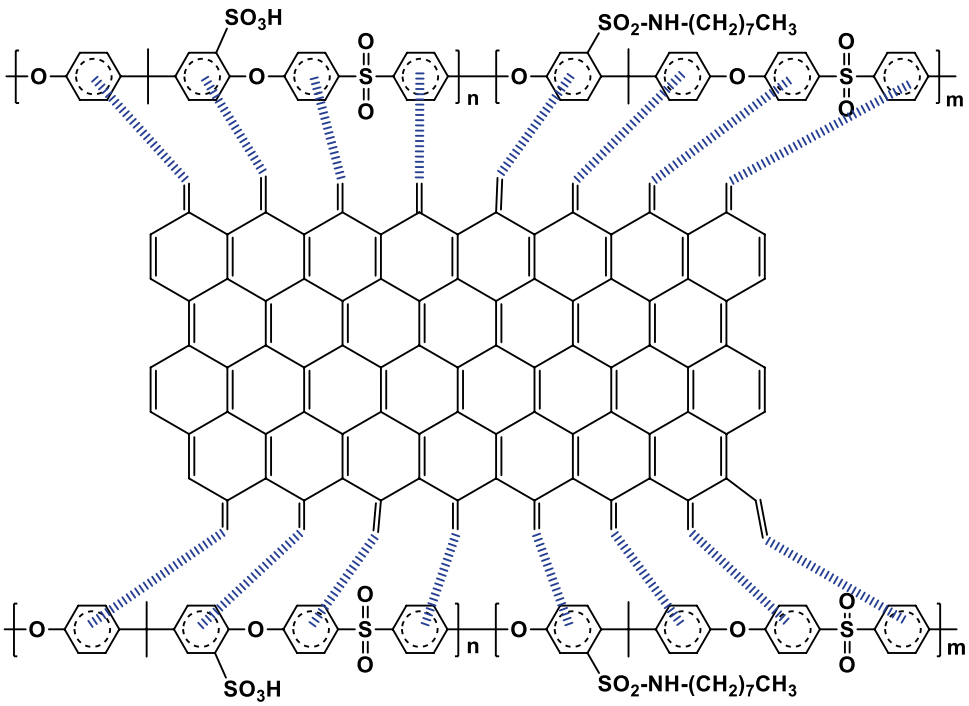

Fig. 1 π–π interaction between the SPESOS matrix and graphene

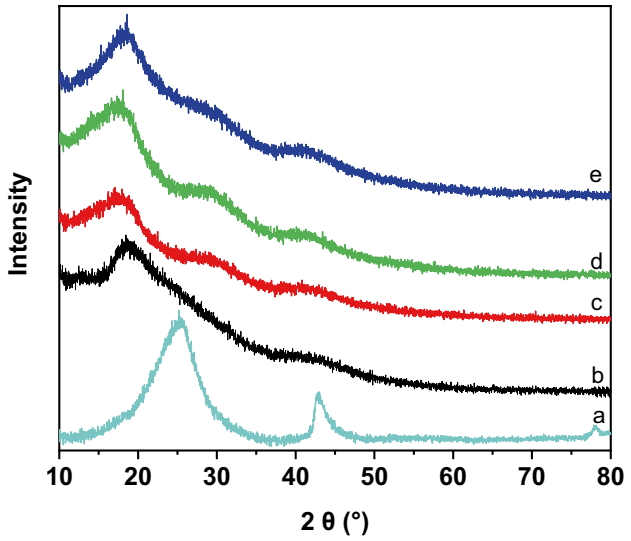

Fig. 3 X-ray diffraction of **a** G, **b** SPESOS, **c** 1 wt.% G/SPESOS, **d** 1.5 wt.% G/SPESOS, and **e** 2 wt.% G/SPESOS hybrid films

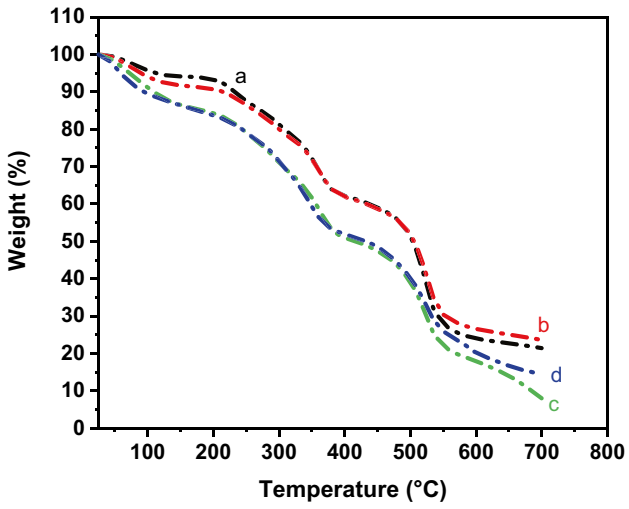

Fig. 4 Thermogravimetric analysis of **a** SPESOS, **b** 1 wt.% G/SPESOS, **c** 1.5 wt.% G/SPESOS, and **d** 2 wt.% G/SPESOS hybrid films

a lower angle (17.47°). Due to the presence of graphene, the diffraction peaks in the hybrid shifted to the lower angles, and the d-spacing on the low-angle side increased (Table 1).

Graphene has a smaller ionic radius than SPESOS and increases the compressive stress, which changes lattice parameters in the SPESOS matrix via π–π stacking interaction with graphene [36].

Thermo gravimetric analysis

The thermograms showed that SPESOS and its hybrids had three stages of mass loss, which occurred between room temperature and 700 °C (Fig. 4). At around 100 °C, the thermograms showed the first stage of degradation, which was due to the initial mass loss caused by the evaporation of water. The degradation of the sulfonated groups responsible for the second substantial mass loss occurred at 200 °C.

The third and final stage of degradation corresponding to a considerable mass loss occurred at about 500 °C and was due to the breakdown of the primary polymer matrix [29]. Due to the smaller weight loss, i.e., 7% at 200 °C, graphene (1 wt.% G/SPESOS) was considered to have higher thermal stability. The hybrids with a higher graphene content, however, demonstrated lower thermal stability, i.e., 18% weight loss at 200 °C. The significant increase in the thermal stability of the hybrid with 1 wt.% graphene might be due to the restricted movement of aromatic backbones as a result of interfacial interactions [34, 37].

Table 1 XRD analysis of SPESOS and its hybrid films

Sample	2θ (°)	d (Å)
SPESOS	19.17	4.68
1% G/SPESOS	17.47	4.87
1.5% G/SPESOS	17.49	5.13
2% G/SPESOS	17.64	5.08

Water uptake

An increase in the water absorption capacity of the hybrid films can improve their proton conductivities via vehicle and Grotthuss mechanisms [30]. The water uptake values of the hybrid films with different ratios of graphene were evaluated after immersing them in deionized water over a weekend (Table 2). Compared to pristine SPESOS films, hybrid films absorb more water. The water uptake capacity of the SPESOS film without graphene was the least (38.8%), whereas the uptake capacities of the hybrids with 1 wt.%, 1.5 wt.%, and 2 wt.% graphene were 41.1%, 42.5%, and 44.5%, respectively. The increase in the uptake capacities might be attributed to the hydrophilicity of the surface of the films. The presence of many hydrophilic groups in SPESOS and graphene was responsible for the swelling of the hybrid films as well [37]. The percentage change in these films was directly related to water uptake. These findings might be attributed to the hydrophilic properties of graphene. These properties are essential for increasing water uptake and reducing dimensional stability due to SPESOS chain relaxation.

Ionic exchange capacity

We found that the hybrid 2 wt.% G/SPESOS had the highest IEC of 2.15 meq/g, indicating the presence of more acidic functionalities (Table 2).

Table 2 Experimental and theoretical IEC values for hybrid films

Sample	Theoretical IEC/(meq/g)	Experimental IEC/(meq/g)	Water uptake/(%)
SPESOS	2.00	1.80	38.9
1 wt.% G/SPESOS	2.00	1.93	41.2
1.5 wt.% G/SPESOS	2.00	1.95	42.5
2 wt.% G/SPESOS	2.00	2.15	44.6

The IEC values of G/SPESOS increased with the amount of graphene. This could be due to the influence of hydrogen bonding and electrostatic interactions between graphene and SPESOS [17, 37]. The difference between the experimental and theoretical values of the ion exchange capacities of the different films might be due to the experimental errors in acid–base titration.

Contact angle

The variations in the contact angles of the hybrids with changes in the amount of graphene are shown in Fig. 5.

The values of contact angles of the films were less than 90°, which indicated good hydrophilicity and wettability. This might be due to the interaction between the sulfonated groups in the pristine SPESOS and graphene (Fig. 5) [33, 34]. These results matched those of thermogravimetric analysis and water uptake evaluation.

Proton conductivity

The influence of temperature and graphene loading on the proton conductivity of the hybrid films was analyzed under 100% hydration conditions (Fig. 6).

We found that the proton conductivity of the various hybrid films remained comparatively low and consistent between ambient temperature and 60 °C. The highest conductivities of 92 and 82 mS/cm were obtained for the hybrid films with 2 and 1.5% of graphene, respectively, while the pure SPESOS film only exhibited proton conductivity of 34 mS/cm at 110 °C. This might be due to the graphene present in the polymer matrix that considerably decreased proton transfer compared to the proton transfer in pristine SPESOS. The quick motion of the conducting sites and the increased activity of sulfonated ions at high temperatures were probably responsible for these results. Graphene, with a high aspect ratio and sheet-like structure, connected the non-covalent clusters through π-π interactions and subtle regions in the SPESOS matrix, which improved the conductivity of the hybrids. An increase in water absorption and swelling of the films allowed proton migration via several π bonds (Fig. 1). The conductivity results for films with a higher graphene content (1.5 and 2 wt.%) were highly encouraging and promising. These results showed that graphene played a key role in increasing the conduction properties of hybrid films owing to their better ability to retain water molecules (proton carriers) at high temperatures. The results of the

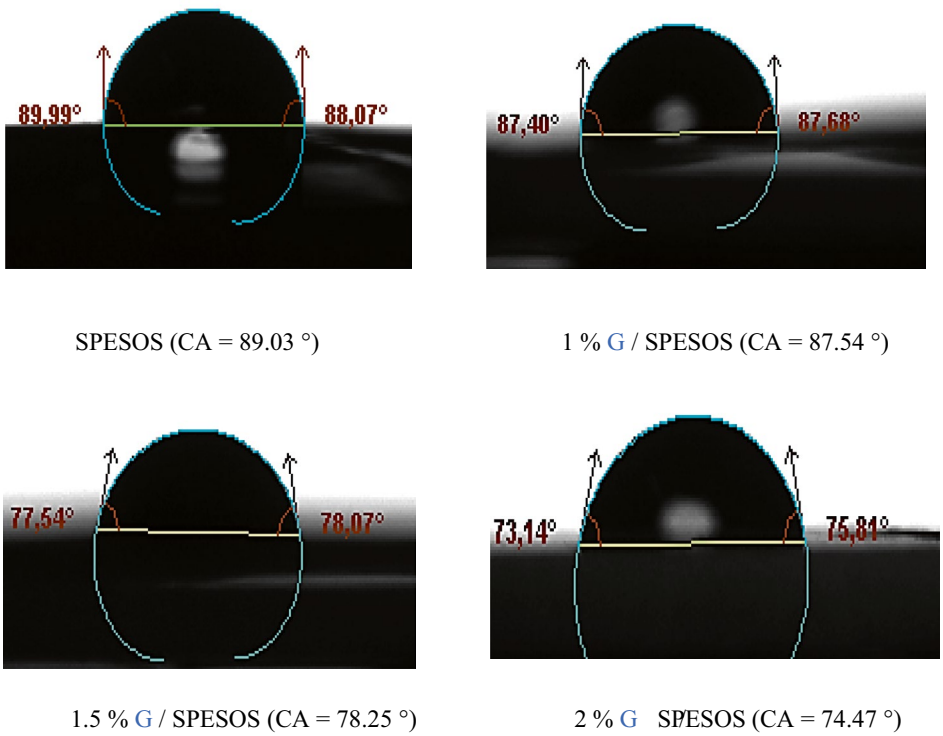

SPESOS (CA = 89.03 °) 1 % G / SPESOS (CA = 87.54 °)

1.5 % G / SPESOS (CA = 78.25 °) 2 % G SPESOS (CA = 74.47 °)

Fig. 5 Comparison between the contact angle values of the hybrid films

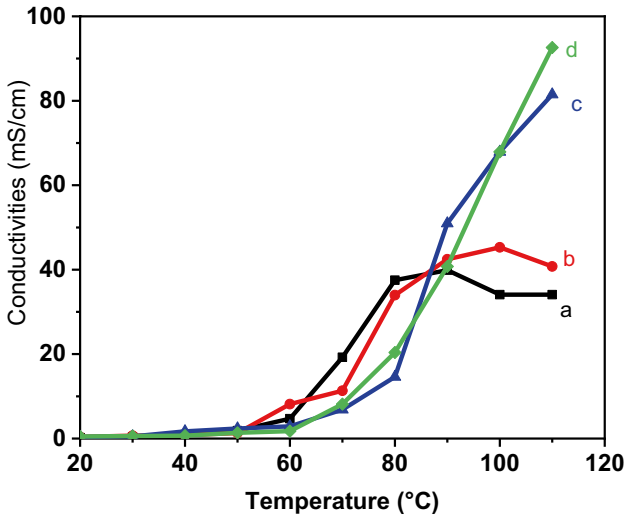

Fig. 6 Proton conductivity of **a** SPESOS, **b** 1 wt.% G/SPESOS, **c** 1.5 wt.% G/SPESOS, and **d** 2 wt.% G/SPESOS hybrid films at 100% RH

electrochemical and thermal analyses presented and discussed above match this conclusion. The activation energy of conduction can be obtained and evaluated by applying the Arrhenius equation:

$$\sigma = \sigma_0 \exp(-E_a/RT) \quad (4)$$

Here, σ and σ_0 indicate the proton conductivity and the pre-exponential factor (S/cm), respectively, R indicates the universal gas constant (8.314472 J/mol. K), and T indicates the absolute temperature (K) [37, 38].

The values of the activation energy of SPESOS and the hybrid films obtained using Eq. (4) at 100% RH are shown in Table 3.

The increase in the percentage of graphene in the matrix of SPESOS resulted in a decrease in the values of activation energy. The addition of graphene influenced the activation energy (E_a), and the lowest value was obtained with 2 wt.% of graphene. This was consistent with the results obtained for higher proton conductivity.

Table 3 The values of activation energy and proton conductivity at 110 °C

Film	Conductivity/(mS/cm) at 110 °C	E_a/(kJ/mol)
SPESOS	**34**	**80.6**
1 wt.% G/SPESOS	41	71.3
1.5 wt.% G/SPESOS	82	6.6
2 wt.% G/SPESOS	92	6.2

Conclusions

A series of G/SPESOS hybrid films was synthesized via solution casting using different ratios of graphene to the polymer. The interactions of the incorporated graphene with the aromatic rings in SPESOS via π-π interactions resulted in the thermal reinforcement of the film and enhanced the mobility of protons to augment the conductivity. Especially, the 2 wt.% G/SPESOS film showed a higher proton conductivity value (92 mS/cm) than the other hybrid films (1 and 1.5 wt.% graphene) and the pristine SPESOS film (34 mS/cm). The thermogravimetric analysis showed excellent thermal stability of the composite membranes. The rate of swelling in the water of the membranes elaborated by the addition of the graphene nanoparticles increased substantially compared to the rate of swelling in the water of the pristine SPESOS membrane.

The composite membranes with contact angles better than those of the pure membrane were obtained. These results are promising. The elaborated membranes might be used in other applications such as electrodialysis, dialysis, and modified electrodes. The approach used might be applied to other polymers and nanoparticles.

Acknowledgements The authors would like to thank Research and Technology Center of Energy, Technopark Borj Cedria for their support. The authors extend their appreciation to the manager of Eras Labo for providing the SPESOS polymer free of charge.

Declarations

Conflict of interest The authors declare no competing interests.

References

1. Sahu AK, Ketpang K, Shanmugam S, Kwon O, Lee SC, Kim H (2016) Sulfonated graphene-Nafion hybrid films for polymer electrolyte fuel cells operating under reduced relative humidity. J Phys Chem C120(29):15855–15866. https://doi.org/10.1021/acs.jpcc.5b11674
2. Vinothkannan M, Kim AR, Nahm KS, Yoo DJ (2016) Ternary hybrid (SPEEK/SPVdF-HFP/GO) based film electrolyte for the applications of fuel cells: profile of improved mechanical strength, thermal stability and proton conductivity. RSC Adv 6(110):108851–108863. https://doi.org/10.1039/C6RA22295A
3. Kim AR, Vinothkannan M,Yoo DJ (2018) Sulfonated fluorinated multi-block copolymer hybrid containing sulfonated(poly ether ether ketone) and graphene oxide: a ternary hybrid film architecture for electrolyte applications in proton exchange film fuel cells. J Energy Chem 27(4):1247–1260. https://doi.org/10.1016/j.jechem.2018.02.020
4. Wu H, Peng T, Kou Z, Cheng K, Zhang J, Zhang J, Meng T, Mu S (2017) In situ constructing of ultrastableceramic@graphene core-shell architectures as advanced metal catalyst supports toward

oxygen reduction. J Energy Chem 26(6):1160–1167. https://doi.org/10.1016/j.jechem.2017.08.012
5. Tian XL, Wang L, Deng P, Chen Y, Xia BY (2017) Research advances in unsupported Pt-based catalysts for electrochemical methanol oxidation. J Energy Chem 26(6):1067–1076. https://doi.org/10.1016/j.jechem.2017.10.009
6. Neelakandan S, Kaleekkal NJ, Kanagaraj P, Sabarathinam RM, Muthumeenal A, Nagendran A (2016) Effect of sulfonated graphene oxide on the performance enhancement of acid-base hybrid films for direct methanol fuel cells. RSC Adv 6(57):51599–51608. https://doi.org/10.1039/C5RA27655A
7. Kim AR, Vinothkannan M, Yoo DJ (2017) Sulfonated-fluorinated copolymer blending films containing SPEEK for use as the electrolyte in polymer electrolyte fuel cell (PEFC). Int J Hydrogen Energy 42(7):4349–4365. https://doi.org/10.1016/j.ijhydene.2016.11.161
8. Park CK, Lee CH, Guiver MD, Lee YM (2011) Sulfonated hydrocarbon films for medium-temperature and low-humidity proton exchange film fuel cells (PEMFCs). Prog Polymer Sci 36(11):1443–1498. https://doi.org/10.1016/j.progpolymsci.2011.06.001
9. Kreuer KD (2001) On the development of proton conducting polymer films for hydrogen and methanol fuel cells. J Membrane Sci 185(1):29–39. https://doi.org/10.1016/S0376-7388(00)00632-3
10. Xing P, Robertson GP, Guiver MD, Mikhailenko SD, Kaliaguine S (2005) Synthesis and characterization of poly(aryl ether ketone) copolymers containing (hexafluoroisopropylidene)-diphenol moiety as proton exchange film materials. Polymer 46(10):3257–3263. https://doi.org/10.1016/j.polymer.2005.03.003
11. Xing P, Robertson GP, Guiver MD, Mikhailenko SD, Wang K, Kaliaguine S (2004) Synthesis and characterization of sulfonated poly(ether ether ketone)forproton exchange films. J Film Sci 229(2):95–106. https://doi.org/10.1016/j.memsci.2003.09.019
12. Kim YS, Einsla B, Sankir M, Harrison W, Pivovar BS (2006) Structure–property–performance relationships of sulfonated poly(arylene ether sulfone)s as apolymer electrolyte for fuel cell applications. Polymer 47(11):4026–4035. https://doi.org/10.1016/j.polymer.2006.02.032
13. Mabrouk W, Ogier L, Matoussi F, Sollogoub C, Vidal S, Dachraoui M, Fauvarque JF (2011) Preparation of new proton exchange films using sulfonated poly (ether sulfone) modified by octylamine (SPESOS). Mater Chem Phys 128(3):456–463. https://doi.org/10.1016/j.matchemphys.2011.03.031
14. Ahmed Z, Charradi K, Alsulami QA, Keshk SMAS, Chtourou R (2021) Physicochemical characterization of low sulfonated polyether ether ketone/smectite clay hybrid for proton exchange film fuel cells. J Appl Polym Sci 138(1):e49634. https://doi.org/10.1002/app.49634
15. Charradi K, Ahmed Z, Thmaini N, Aranda P, Al-Ghamdi YO, Ocon P, Keshk SAMS, Chtourou R (2021) Incorporation of layered double hydroxide/sepiolite to improve the performance of sulfonated poly(ether ether ketone) hybridfilms for proton exchange film fuel cells. J Appl Polym Sci 138(19):e50364. https://doi.org/10.1002/app.50364
16. Mabrouk W, Charradi K, Lafi R, AlSalem HS, Meherzi HM, Keshk SAMS (2022) Incorporation of sepiolite clay within sulfonated polyether sulfone octyl sulfonamide for the augmentation of proton conductivity. J Mater Sci 57(140):15331–15339. https://doi.org/10.1007/s10853-022-07627-5
17. Mabrouk W, Charradi K, Meherzi HM, Alhussein A, Keshk SAMS (2022) Proton conductivity amelioration of sulfonated poly ether sulfone octyl sulfonamide via the incorporation of Montmorillonite. J Electron Mater 51(139):6369–6378. https://doi.org/10.1007/s11664-022-09862-7
18. Pushparaj VL, Shaijumon MM, Kumar A, Murugesan S, Ci L, Vajtai R, Linhardt RJ, Nalamasu O, Ajayan PM (2007) Flexible energy storage devices based on nanohybrid paper. Proc Natl Acad Sci 104(39):13574–13577. https://doi.org/10.1073/pnas.070650810
19. Chen J, Minett AI, Liu Y, Lynam C, Sherrell P, Wang C, Wallace GG (2008) Direct growth of flexible carbon nanotube electrodes. Adv Mater 20(3):566–570. https://doi.org/10.1002/adma.200701146
20. Chou SL, Wang JZ, Chew SY, Liu HK, Dou SX (2008) Electrodeposition of MnO_2 nanowires on carbon nanotube paper as free-standing, flexible electrode for supercapacitors. Electrochem Commun 10(11):1724–1727. https://doi.org/10.1016/j.elecom.2008.08.051
21. Mathew E, Manoj B (2022) Disorders in graphene: types, effects and control techniques-a review. Carbon Lett 32(240):431–450. https://doi.org/10.1007/s42823-021-00289-4
22. Yoo E, Kim J, Hosono E, Zhou H, Kudo T, Honma I (2008) Large reversible Li storage of graphene nanosheet families for use in rechargeable lithium ion batteries. Nano Lett 8(8):2277–2282. https://doi.org/10.1021/nl800957b
23. Yin H, Zhang C, Liu F, Hou Y (2014) Hybrid of iron nitride and nitrogen-doped graphene aerogel as synergistic catalyst for oxygen reduction reaction. Adv Funct Mater 24(20):2930–2937. https://doi.org/10.1002/adfm.201303902
24. Ye YS, Cheng MY, Xie XL, Rick J, Huang YJ, Chang FC, Hwang BJ (2013) Alkali doped polyvinyl alcohol/graphene electrolyte for direct methanol alkaline fuel cells. J Power Sources 239:424–432. https://doi.org/10.1016/j.jpowsour.2013.03.021
25. Wang S, Yu D, Dai L, Chang DW, Baek JB (2011) Polyelectrolyte-functionalizedgraphene as metal-free electrocatalysts for oxygen reduction. ACS Nano 5(8):6202–6209. https://doi.org/10.1021/nn200879h
26. Yong YC, Dong XC, Chan-Park MB, Song H, Chen P (2012) Macroporous and monolithic-anode based on polyaniline hybridized three-dimensional graphene for high-performance microbial fuel cells. ACS Nano 6(3):2394–2400. https://doi.org/10.1021/nn204656d
27. Dai W, Yu L, Li Z, Yan J, Liu L, Xi J, Qiu X (2014) Sulfonated poly(ether ether ketone)/graphene hybrid film for vanadium redox flow battery. Electrochi Acta 132:200–207. https://doi.org/10.1016/j.electacta.2014.03.156
28. Xiaobing H, Hao K, Tao C, Jie G, Yuan Z, Sang Y, Guowen H (2021) Effect of π–π stacking interfacial interaction on the properties of graphene/poly(styrene-b-isoprene-b-styrene) hybrids. Nanomaterials 11(9):2158. https://doi.org/10.3390/nano11092158
29. Choi E, Han TH, Hong J, Kim J, Lee SH, Kima HW (2010) Noncovalent functionalization of graphene with end-functional polymers. J Mater Chem 20(9):1907–1912. https://doi.org/10.1039/B919074K
30. Mabrouk W, Lafi R, Charradi K, Ogier L, Hafiane A, Fauvarque JF, Sollogoub C (2020) Synthesis and characterization of new proton exchange film deriving sulfonated polyether sulfone using ionic crosslinking electrodialysis applications. Polym Eng Sci 60(12):3149–3158. https://doi.org/10.1002/pen.25543
31. Charradi K, Ahmed Z, Moussa M, Beji Z, Brahmia A, Othman I, Abu-Haija M, Chtourou R, Keshk SM (2022) A facile approach for the synthesis of zinc ferrite/cellulose as an effective magnetic photocatalyst for the degradation of methylene blue in aqueous solution. Cellulose 29(466):2565–2576. https://doi.org/10.1007/s10570-021-04334-3
32. Bagheri A, Javanbakht M, Beydaghi H, Salarizadeh P, Shabanikiac A, Amoli HS (2016) Sulfonated poly(ether ether ketone) and sulfonated polyvinylidene fluoride-co-hexafluoropropylene based blend proton exchange films for direct methanol fuel cell applications. RSC Adv 6(45):39500–39510. https://doi.org/10.1039/C6RA00038J
33. Liang L, Shi Z, Tan X, Sun S, Chen M, Dastan D, Dong B, Cao L (2021) Largely improved breakdown strength and discharge efficiency of layer-structured nanocomposites by filling with a small loading fraction of 2D zirconium phosphate nanosheets. Adv Mater Interfaces 9:2101646. https://doi.org/10.1002/admi.202101646

34. Zhang M, Shi Z, Zhang J, Zhang K, Lei L, Dastan D, Dong B, Cao L (2021) Greatly enhanced dielectric charge storage capabilities of layered polymer composites incorporated with low loading fractions of ultrathin amorphous iron phosphate nanosheets. J Mater Chem C 9:10414–10424. https://doi.org/10.1039/DITC01974K
35. Liu Y, Wang J, Zhang H, Ma C, Liu J, Cao S, Zhang X (2014) Enhancement of proton conductivity of chitosan film enabled by sulfonated graphene oxide under both hydrated and anhydrous conditions. J Power Sources 269:898–911. https://doi.org/10.1016/j.jpowsour.2014.07.075
36. Mabrouk W, Lafi R, Fauvarque JF, Hafiane A, Sollogoub C (2021) New ion exchange film derived from sulfochloratedpolyether sulfone for electrodialysis desalination of brackish water. Polym Adv Technol 32(1):304–314. https://doi.org/10.1002/pat.5086
37. Altaf F, Ahmed S, Dastan D, Batool R, Rehman ZU, Shi Z, Hameed MU, Bocchetta P, Jacob K (2022) Novel sepiolite reinforced emerging composite polymer electrolyte membranes for high-performance direct methanol fuel cells. Mater Today Chem 24:100843. https://doi.org/10.1016/j.mtchem.2022.100843
38. Zhu P, Dastan D, Liu L, Wu LK, Shi Z, Chu QQ, Altaf F, Mohammed MKA (2023) Surface wettability of various phases of titania thin films: atomic-scale simulation studies. J Mol Graph Model 118:108335. https://doi.org/10.1016/j.jmgm.2022.108335